

Interpreting Fluorescence Microscopy Images and Measurements

Jennifer C. Waters¹ and Jason R. Swedlow^{2,*}

¹Department of Cell Biology, Harvard Medical School, 240 Longwood Avenue, Boston, MA 02115, USA

²Wellcome Trust Centre for Gene Regulation and Expression, MSI/WTB/JBC Complex, College of Life Sciences, University of Dundee, Dow Street, Dundee DD1 5EH, Scotland

*Correspondence: jason@lifesci.dundee.ac.uk

Introduction

Fluorescence microscopy images grace the covers of many of the scientific journals delivered to our desk or email inbox. However, these images are much more than just pretty pictures. Opening any cell biology journal reveals that fluorescence images are critical data, increasingly used as results for quantitative assays. This is possible because fluorescence microscopy provides a spatially and temporally resolved measurement of the concentration of multiple molecules in cells, tissues, and even whole animals. The wide variety of molecularly specific labels, including genetically encoded fluorescent proteins (Giepmans et al., 2006), and a range of new imaging techniques and modalities have transformed fluorescence microscopy from a simple localization test to a suite of quantitative tools for functional analysis. Given the broad use of fluorescence microscopy and the pace of development of new methodologies, it has become important for most biologists to be able to critically evaluate fluorescence images and quantitative analysis. Unfortunately, many published images cannot accurately represent the original specimen, so an understanding of how the sample under the microscope was transformed into the published image can be difficult.

The methods used for imaging a fixed antibody-stained embryo differ greatly from those used in a live cell Förster resonance energy transfer experiment. Regardless of the sample or imaging method, a successful imaging experiment requires achieving sufficient resolution and signal-to-noise ratio (SNR) to obtain a definitive result. The SNR varies greatly depending on the imaging system, and determines the minimum level of detectable fluorescence (Pawley, 2006; Swedlow et al., 2002; Murray et al., 2007). Collecting images with high signal and low noise is especially important for quantitative fluorescence microscopy, as images with poor SNR will yield less accurate quantitative results. In this minireview, we discuss the various technical considerations for an imaging experiment in terms of their effects on resolution and SNR. We include brief descriptions of the methods and issues for consideration when reading a paper that uses imaging, but the interested reader is referred to a number of thorough and authoritative resources (Davidson, 2007; Pawley, 2006; Goldman and Spector, 2005; Inoué and Spring, 1997). In addition, a number of intensive courses are available at sites around the world that will provide detailed coverage and discussion of the issues we cover in this article.

Spatial Resolution

The spatial resolution in a microscope image is defined as the ability to distinguish two separate objects as separate (Inoué and Spring, 1997). The resolution limit in the image plane is defined as

$$d = \frac{1.22\lambda}{NA_{\text{objective}} + NA_{\text{condenser}}}$$

where d is the minimal resolvable distance, λ is the wavelength, and NA is the numerical aperture (note that in fluorescence microscopy, the objective acts as the condenser). For fluorescence microscopy, the resolution limit along the optical axis is defined as

$$d = \frac{2\lambda n}{NA_{\text{objective}}^2}$$

where n = refractive index of the mounting media. These limits are especially important when performing distance measurements.

The easiest way to visualize these limits is with fluorescent beads that are substantially smaller than the resolution limit (usually diameter ≤ 200 nm; Figure 1). A three-dimensional image of a single bead reports the blurring (or point-spread function; PSF) that is stamped on every object by the objective lens (for a full treatment, see Goodman, 1996). Using a highest-resolution objective lens to image green light, the full width of the PSF of a standard fluorescence microscope at half its maximal intensity (FWHM) will be ~ 250 nm in the image plane and ~ 700 nm along the optical axis. This substantial difference in axial resolution (and concomitant increase in blurring) is a normal feature of all light microscopes and complicates distance measurements in images of 3D objects.

Both of these treatments are based on the size of the PSF. An alternative form of defining spatial resolution involves the precision of measuring the center of mass of an object. As the PSF is a Gaussian, its center can be estimated with subnanometer precision. This approach is the basis for single-particle tracking (Qian et al., 1991). Single-particle tracking is commonly used for single-molecule analysis and is increasingly applied to define the mechanical properties of resolution-limited structures inside the cell.

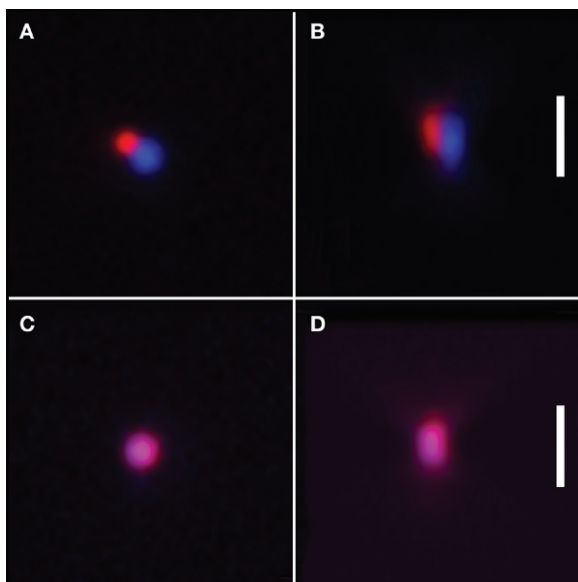


Figure 1. Fluorescent Beads Reveal the Point-Spread Function and Aberrations

Images of 170 μm spherical beads that fluoresce both blue and red (TetraSpeck beads, Invitrogen/Molecular Probes). Z series images were collected, with both wavelengths collected at each focal plane. (A) and (B) were collected with a PlanApo 100 \times 1.4 NA objective lens. (C) and (D) were taken with a second PlanApo 100 \times 1.4 NA objective lens from the same manufacturer. (A) and (C) are lateral X, Y pseudocolored and overlaid images. In (B) and (D), 3D X, Z reconstructions reveal the axial images, also pseudocolored and overlaid. Note that the axial resolution is worse than the lateral resolution, as is shown by the elongated shape of the spherical bead in Z.

(A and B) Lateral axial chromatic aberration in the objective lens causes a shift between wavelengths.

(C and D) The second lens has near-negligible chromatic aberration. Comparison of (A) and (B) with (C) and (D) demonstrates the range of aberration correction found in PlanApo lenses.

The scale bars represent 1 μm .

The Objective Lens

Of the many choices that must be made in fluorescence imaging, one of the most critical to resolution and SNR is the objective lens (Inoué and Spring, 1997). All papers using fluorescence microscopy should specifically state the magnification, numerical aperture (NA), and any specific characteristics of the objective lens(es) used. Magnification simply states the magnification of the specimen onto the image plane. NA is a measure of the acceptance angle of the objective lens and, as described above, is directly related to the lateral and axial resolution limits. A larger NA means a larger acceptance angle, and thus a brighter lens. All other elements being equal, the brightness of a lens varies with NA^4 in fluorescence microscopy, so NA has significant effects on both resolution and SNR. Choosing an objective lens that collects and transmits as much light as possible is vital to attaining a high SNR. This must be considered when mounting the specimen, as the highest NA objective lenses require immersion oil and the specimen to be grown on a number 1.5 coverslip.

Aberrations inherent in the refractive lenses used in objectives can deteriorate resolution and degrade SNR. Different lenses are corrected to different degrees (Inoué and Spring, 1997), and the degree of correction is always marked on the barrel of the objective. Correction for two of the most common problems, chromatic aberration (Figure 1) and spherical aberration (Figure 2), is indicated by achromatic (least corrected), fluorite, and apochromatic (most corrected). Unfortunately, correction for aberrations also decreases the transmission of light through the lens, decreasing the signal in the image. Therefore, there are tradeoffs between degree of correction and SNR.

Chromatic aberrations affect colocalization and therefore any measurements between two wavelengths. Chromatic aberration generates a systematic displacement of signal in one wavelength signal relative to another, and can occur in the image plane or along the optical axis (Figures 1A and 1B). Axial chromatic aberrations occur because different wavelengths of light refract at different angles as they leave the lens, causing them to focus at different planes. Chromatic aberration is variable in the most highly apochromat corrected lens (Figures 1A and 1B), as a shift between most wavelengths of up to 500 nm is considered to be within the apochromat specification. Achieving this type of correction is a remarkable engineering feat, but may be insufficient for high-resolution colocalization. For studies that require colocalization of objects near the resolution limit of the microscope, shifts between wavelengths should be measured using commercially available multicolor fluorescent beads less than 200 nm in diameter (Invitrogen/Molecular Probes, Carlsbad, CA, USA). Once measured, the shift can be corrected for using most image-processing software packages.

Spherical aberration appears as asymmetry in the out-of-focus light above and below the focal plane (i.e., brighter when focusing up and dimmer when focusing down, or vice versa) and degrades SNR and axial resolution (Figure 2) (Hell et al., 1993; Hiraoka et al., 1990). Spherical aberration occurs in objective lenses because light rays that pass through the center of the lens come into focus at a different plane than rays that pass through the periphery of the lens, resulting in an axial elongation of the image. Spherical aberration can also be introduced by the specimen. This most commonly occurs because of a mismatch of refractive index between the medium surrounding the specimen and the lens immersion medium, or because of an error in coverslip thickness (Hiraoka et al., 1990; Wallace et al., 2001). For low light level imaging, or imaging in which axial resolution must be maximized, spherical aberration should be addressed. Fixed specimens should be mounted in media containing high levels of glycerol or other high-refractive index material. When imaging a specimen mounted in an aqueous medium using an oil immersion objective lens, spherical aberration changes

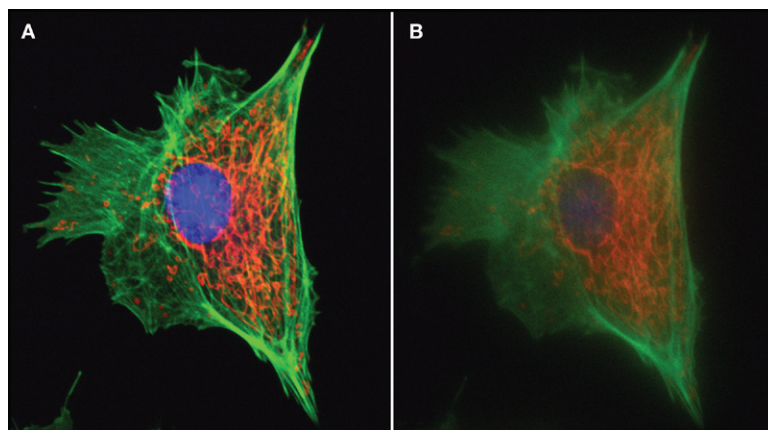


Figure 2. Comparison of Image Quality without and with Spherical Aberration

Images are BSC-1 cells with labeled DNA (blue), actin (green), and mitochondria (red).

(A) A lens with minimal spherical aberration produces a crisp, bright image.

(B) Spherical aberration was introduced using immersion oil of higher refractive index to create a greater change in refractive index between the specimen and immersion media. This mimics the change in refractive index between immersion oil and aqueous cell-culture media.

with focus position, so critical 3D distance measurements can contain errors. Spherical aberrations can be minimized by adjusting the refractive index of the immersion oil (Hiraoka et al., 1990) or by using an objective lens that is designed for an immersion medium that matches the mounting medium. The availability of high-NA water immersion lenses has helped minimize spherical aberration in live specimens in aqueous cell-culture media, although these lenses require careful sample mounting to prohibit the introduction of artifacts (Arimoto and Murray, 2004).

Choosing between Modes of Microscopy

There are several different modes of fluorescence microscopy, each of which will produce a different image of the same specimen. Some of the most common modes include wide-field, confocal (including spinning disk confocal and laser scanning confocal), multiphoton, and total internal reflection fluorescence (TIRF). The term wide-field fluorescence is used to describe standard fluorescence microscopy, in which the entire field of view is illuminated and all fluorescence (both in and out of focus) is collected. Point scanning confocal microscopy (also called laser scanning confocal) uses a focused light source to scan the image point by point and a pinhole at the image plane to block out-of-focus fluorescence from reaching the detector. Multipoint or slit scanning confocals (such as the spinning disk confocal) use multiple pinholes or slits to more quickly illuminate the specimen and remove out-of-focus information. In multiphoton, the specimen is illuminated with a high-power long-wavelength laser, resulting in excitation of the fluorophores through absorption of multiple photons at the same time. In TIRF microscopy, the fluorophores are excited with the evanescent wave of energy that forms when total internal reflection occurs at the boundary between media of different refractive indexes, namely the coverslip and the specimen.

There is no one fluorescence microscopy technique that is “the best.” Instead, the different modes are more or less appropriate for different samples and

experimental requirements. The best choice depends on the specimen and the type of information that is needed. It is critical to determine which technique will provide sufficient SNR, resolution, and temporal resolution for the experiment (Murray, 2004; Murray et al., 2007).

The benefit of confocal over wide-field microscopy is the removal of out-of-focus information and thus improved SNR. A common misconception is that confocal should be used whenever a high-resolution image is desired. Although confocal imaging can result in a modest increase in resolution, it is rarely enough to reveal biological structure that would be missed by wide-field fluorescence. Standard laser scanning confocal works well for imaging up to approximately 50 μm into a thick specimen, after which the loss of SNR (due primarily to light scattering) may be inhibiting (Murray, 2004). Multiphoton is preferable for specimens that are thicker than 100 μm , as the long wavelengths of light used to illuminate the specimen penetrate deep into biological specimens, and emitted light that is scattered by the specimen can be collected and used for image formation (Denk and Svoboda, 1997).

Multipoint (such as the spinning disk confocal) or slit scanners have the benefit of faster acquisition and low noise, making them favorable for live cell work. Their limitation is the size of the pinhole or slit, which may allow some out-of-focus light through. The most commonly used model of spinning disk confocal (made by Yokogawa) is limited by a fixed pinhole size, which is optimized for removal of out-of-focus fluorescence only with a 100 \times 1.4 NA objective lens. Using this instrument with an objective lens with lower magnification results in more out-of-focus light in the image.

TIRF (Axelrod, 2001) produces the thinnest possible optical section, on the order of 50–100 nm compared with approximately 700 nm for confocal. This results in a very high SNR image. The caveat is that the specimen is only illuminated at the coverslip surface, making TIRF useful for a limited number of applications such as imaging of the plasma membrane, focal adhesions, and in vitro assays.

The choice between these different modes of microscopy depends ultimately on the sources of noise both in the sample and in the microscope instrumentation (Murray et al., 2007). The best choice for a particular experiment can often only be determined by a direct comparison of the same sample on different microscopes (Swedlow et al., 2002; Zucker and Price, 2001).

Two-Dimensional or Three-Dimensional?

Cells and tissues are three-dimensional objects, whereas light microscopes record two-dimensional images. The advent of optical sectioning fluorescence microscopy (Agard and Sedat, 1983) enabled the generation of 3D images from a series stack of 2D images taken at a defined focus interval. A common misconception is that a confocal microscope is necessary to create a 3D image. In fact, any microscope that allows images to be recorded at defined focus intervals, or “optical sections,” can generate 3D images. As discussed above, the axial resolution is limited by the NA, so the effective depth of an optical section is also limited by NA. For objects moving in 3D, distance measurements should be made on 3D stacks of images. Fluorescence intensity measurements made on objects that extend beyond a single optical section should also be performed in 3D so that effects of object blurring along the optical axis can be taken into account. This is especially important in live cell imaging, where an object’s 3D orientation may change during data acquisition.

Live Cell Imaging with Limited SNR

It is especially difficult to obtain a high SNR when imaging live specimens. For live cell imaging, it is common to choose cells with minimal fluorophore (i.e., cells that are weakly expressing fluorescent protein conjugates, to minimize overexpression artifacts) and to minimize illumination to decrease phototoxicity and bleaching. These choices limit SNR, but this is often a worthwhile compromise to ensure specimen viability and success of the experiment. However, it is important to remember that images with poor SNR will yield quantitative results with reduced accuracy and precision.

Temporal Sampling

When performing time-lapse imaging of living cells or tissues, exposure times must be short enough so that significant movement does not occur during an exposure. In addition, it is important that images are collected frequently enough to properly capture movement or fluorescence changes. A recent study has highlighted this issue in the study of yeast microtubule dynamics (Dorn et al., 2005). For experiments where fluorescence signal is perturbed and the response is then recorded (for example, fluorescence recovery after photobleaching, FRAP), rapid image acquisition may be required to properly sample the movements that occur in living cells. In addition, when recording optical sections, the length of time it takes to collect each stack of optical sections

should be compared with the timescale of the movements under study. If these are similar, then significant motion will occur across a series of optical sections, which will add errors to any 3D measurements. For very fast processes such as cells flowing through blood vessels, this problem is unavoidable, and can be computationally corrected (Liebling et al., 2005).

Keeping Live Cells Healthy on the Microscope

Imaging is always a stress on live specimens. Shorter wavelengths (like the blue light used to excite GFP) cause cell damage even in the absence of fluorophores (see Swedlow et al., 2004), and fluorophore excitation generates potentially harmful reactive free radicals. Finally, temperature regulation and media buffering are critical for maintaining cell health during imaging. All live cell experiments must include controls demonstrating that cells are relatively healthy; mitotic index and duration of mitosis are good measures of viability (Swedlow et al., 2004).

As described above, it is often necessary to sacrifice SNR in order to minimize exposure of the specimen to light. Camera binning (the pooling together of signal collected by adjacent pixels prior to readout) can be used to increase SNR during live cell imaging (Inoué and Spring, 1997). The tradeoff is a loss of spatial resolution, which for many specimens is a necessary compromise.

Processing and Analyzing Fluorescence Images

Image processing is used to correct for problems such as uneven illumination and to enhance images for further analysis, display, and publication. Image enhancements such as scaling, brightness, contrast, and gamma can be very useful for bringing out the important parts of the image. If two or more images are to be compared, the same processing routine must be applied to each image. Most importantly, a reader should never be expected to judge differences in intensity solely on the basis of displayed images; intensity values should be measured. In the following, we briefly discuss some common image-processing applications and their use. The interested reader is referred to the primary references for more information.

Flat-Field Correction

Almost all image-analysis approaches assume even illumination across the field of view and equal detector response at each point (or pixel) in the image. Illumination gradients are quite common and must be corrected before any signal intensity measurements are made. Tools for performing such flat-field corrections (Wolf, 2003) are included in most image-processing programs.

Photobleaching

Photobleaching is the irreversible destruction of a fluorophore that can occur when the fluorophore is in the excited state. When multiple images of the same field are recorded (as in time-lapse imaging), the signal may decrease because of photobleaching. The rate of photobleaching depends on the fluorophore and intensity of

illumination. Photobleaching should be measured in a control specimen and then corrected for in the images to be analyzed.

Deconvolution

Deconvolution is a computational method of removing or reassigning out-of-focus information postacquisition (McNally et al., 1999; Wallace et al., 2001). There are a wide range of deconvolution algorithms available that produce an equally wide range of results. Most importantly, deconvolution that produces quantitative results (namely constrained iterative methods) must be used when quantitative measurements are to be made (Swedlow et al., 2002).

Regions of Interest

A common approach to image analysis is to use imaging software to segment those regions that will be analyzed. For small data sets, this is sometimes accomplished by simply outlining the regions of interest (ROIs) manually. This can be cumbersome for larger sets of data, and there are a variety of automatic methods for defining ROIs. These regions can then be further analyzed or classified based on properties such as shape and size or signal characteristics. There are a large number of tools available in both open and commercial form that can be surveyed for the best performance with a specific type of data (Tvarusko et al., 2005). In all cases, the same selection criteria should be applied to both control and experimental images.

Background Subtraction

All intensity measurements are a mixture of signal and background, so subtraction of the background is necessary before any further measurements can take place. This is best done by measuring the local background surrounding the signal of interest. The background-corrected fluorescence in the object can be calculated as follows:

$$F_{obj} = \sum_{i=1}^{i=N_{obj}} F_{obj_i} - N_{obj} \frac{\sum_{j=1}^{j=N_{bkg}} F_{bkg_j}}{N_{bkg}}$$

where F is the fluorescence signal measured at each pixel i or j , obj is the object, bkg is the selected background area or volume, and N is the number of pixels in the selected object or background. This equation sums the fluorescence in an object, then calculates the background contribution per pixel. It then corrects the summed object fluorescence by the number of pixels in the object multiplied by background per pixel.

Colocalization

For colocalization studies, separate monochrome images should be shown, as differences in SNR between images may make colocalization hard to visualize in a color overlay. Color overlays should not be relied upon to prove colocalization. Quantitative analysis (line plots, % overlap, or crosscorrelation) should be used to measure overlap between images.

Projections

When 3D images have been collected, published versions of the images are displayed as individual planes or as projections. The type of z projection used should be stated. Maximum-intensity z projections (MIPs) are most often used for fluorescence images, where each pixel in the resulting image is the pixel of maximum intensity in the z series. These produce high-contrast images, but are generated by a nonlinear transformation, so MIPs cannot be used for quantitative analysis.

Reporting Variations and Uncertainties

It is axiomatic that all quantitative measurements should include an estimate of the error or variance in the measurement. In imaging, there are a number of sources of uncertainty in intensity measurements, including photon-counting (Poisson) noise and various forms of illumination and detector noise (Inoué and Spring, 1997). All of these sources of noise will be components of the image. In fluorescence, it is common to measure the signal contained in a series of ROIs and compare them quantitatively. In most cases, the mean signal for a given ROI is averaged with similar measurements from other images. However, there is an uncertainty in the determination of the mean of each ROI, which is usually higher in images of live cells. Intensity measurements on live cell images will almost always be noisier than those measured from fixed cells, as image SNR is usually sacrificed in favor of specimen viability. Whenever mean intensity values are calculated, the standard error of the mean (SEM) should also be calculated (Mandel, 1984). The SEM then accounts for any variation in the signal measured at an individual ROI and can be propagated through any further calculations.

Specifications for Published Images

This review is a survey of the critical issues in reading the methods and results of a paper that uses biological imaging. All of the information described above should be accessible to the reader in the methods section, figure legends, or supplementary material. However, this invariably amounts to a large volume of information in an unstructured format that is difficult for authors to collate, for reviewers and readers to read, and for journals to publish. Our preferred approach would be a standardized format, readable by freely available software, that would include all of the data and methods, available at an author's or another site. A specification for an image file format for light microscopy known as OME-XML has recently been published (Goldberg et al., 2005), and a derivative of this based on the widely used tagged image file format (TIFF) known as OME-TIFF is now available (<http://www.loci.wisc.edu/ome/ome-tiff.html/>). A Java library providing tools for conversion from most commercial file formats to OME-TIFF has also been released (<http://www.loci.wisc.edu/ome/formats.html/>). Use of these formats and support for them by imaging software companies and journals can only help the exchange of critical results and methods within the community of cell and developmental biologists.

Conclusions

Images can provide visually striking results, but they must be critically evaluated like all other data in a paper. As imaging techniques become more specialized, the necessity to evaluate technical details grows. We have described the basic parameters that should be considered when reading papers that use analytical imaging. For further information, we refer the reader to any of the reference books in the bibliography and possibly any of the excellent imaging courses that are held worldwide at many sites—there is nothing like hands-on learning. Happy reading!

ACKNOWLEDGMENTS

We thank the academic and commercial faculty and the students of the Analytical and Quantitative Light Microscopy Course at the Marine Biological Laboratory (http://www.mbl.edu/education/courses/special_topics/aqlm.html) and the Immunocytochemistry, In Situ Hybridization, and Live Cell Imaging Course at Cold Spring Harbor Laboratory (<http://meetings.cshl.edu/courses/c-situ07.shtml>), especially Shinya Inoue, John Murray, Ted Salmon, Kip Sluder, Ken Spring, and David Wolf, for many years of critical discussions on the use of microscopes as quantitative instruments. J.R.S. is a Wellcome Trust Senior Research Fellow.

REFERENCES

- Agard, D., and Sedat, J. (1983). Three-dimensional architecture of a polytene nucleus. *Nature* 302, 676–681.
- Arimoto, R., and Murray, J.M. (2004). A common aberration with water-immersion objective lenses. *J. Microsc.* 216, 49–51.
- Axelrod, D. (2001). Total internal reflection fluorescence microscopy in cell biology. *Traffic* 2, 764–774.
- Davidson, M.J. (2007). *Optical Microscopy Primer* (<http://micro.magnet.fsu.edu/primer/>).
- Denk, W., and Svoboda, K. (1997). Photon upmanship: why multiphoton imaging is more than a gimmick. *Neuron* 18, 351–357.
- Dorn, J.F., Jaqaman, K., Rines, D.R., Jelson, G.S., Sorger, P.K., and Danuser, G. (2005). Yeast kinetochore microtubule dynamics analyzed by high-resolution three-dimensional microscopy. *Biophys. J.* 89, 2835–2854.
- Giepmans, B.N., Adams, S.R., Ellisman, M.H., and Tsien, R.Y. (2006). The fluorescent toolbox for assessing protein location and function. *Science* 312, 217–224.
- Goldberg, I.G., Allan, C., Burel, J.-M., Creager, D., Falconi, A., Hochheiser, H.S., Johnston, J., Mellen, J., Sorger, P.K., and Swedlow, J.R. (2005). The Open Microscopy Environment (OME) data model and XML file: open tools for informatics and quantitative analysis in biological imaging. *Genome Biol.* 6, R47.
- Goldman, R.D., and Spector, D.L., eds. (2005). *Live Cell Imaging: A Laboratory Manual* (Cold Spring Harbor, NY: Cold Spring Harbor Laboratory Press).
- Goodman, J.W. (1996). *Introduction to Fourier Optics* (New York: McGraw-Hill).
- Hell, S., Reiner, G., Cremer, C., and Stelzer, E.H.K. (1993). Aberrations in confocal fluorescence microscopy induced by mismatches in refractive index. *J. Microsc.* 169, 391–405.
- Hiraoka, Y., Sedat, J.W., and Agard, D.A. (1990). Determination of three-dimensional imaging properties of a light microscope system. *Biophys. J.* 57, 325–333.
- Inoué, S., and Spring, K.R. (1997). *Video Microscopy, Second Edition* (New York: Plenum Press).
- Liebling, M., Forouhar, A.S., Gharib, M., Fraser, S.E., and Dickinson, M.E. (2005). Four-dimensional cardiac imaging in living embryos via postacquisition synchronization of nongated slice sequences. *J. Biomed. Opt.* 10, 054001.
- Mandel, J. (1984). *The Statistical Analysis of Experimental Data* (Mineola, NY: Dover Publications).
- McNally, J.G., Karpova, T., Cooper, J., and Conchello, J.A. (1999). Three-dimensional imaging by deconvolution microscopy. *Methods* 19, 373–385.
- Murray, J.M. (2004). Confocal microscopy, deconvolution, and structured illumination methods. In *Live Cell Imaging: A Laboratory Manual*, R.D. Goldman and D.L. Spector, eds. (Cold Spring Harbor, NY: Cold Spring Harbor Laboratory Press), pp. 239–279.
- Murray, J.M., Appleton, P.L., Sedlow, J.R., and Waters, J.C. (2007). Evaluating performance in three-dimensional fluorescence microscopy. *J. Microsc.* 228, 390–405.
- Pawley, J.B. (2006). Fundamental limits in confocal microscopy. In *Handbook of Biological Confocal Microscopy*, J.B. Pawley, ed. (New York: Springer), pp. 20–41.
- Qian, H., Sheetz, M.P., and Elson, E.L. (1991). Single particle tracking. Analysis of diffusion and flow in two-dimensional systems. *Biophys. J.* 60, 910–921.
- Swedlow, J.R., Hu, K., Andrews, P.D., Roos, D.S., and Murray, J.M. (2002). Measuring tubulin content in *Toxoplasma gondii*: a comparison of laser-scanning confocal and wide-field fluorescence microscopy. *Proc. Natl. Acad. Sci. USA* 99, 2014–2019.
- Swedlow, J.R., Andrews, P.D., and Platani, M. (2004). In vivo imaging of mammalian cells. In *Live Cell Imaging: A Laboratory Manual*, R.D. Goldman and D.L. Spector, eds. (Cold Spring Harbor, NY: Cold Spring Harbor Laboratory Press), pp. 329–343.
- Tvarusko, W., Mattes, J., and Eils, R. (2005). Analyzing live cell data and tracking dynamic movements. In *Live Cell Imaging: A Laboratory Manual*, R.D. Goldman and D.A. Spector, eds. (Cold Spring Harbor, NY: Cold Spring Harbor Laboratory Press), pp. 303–326.
- Wallace, W., Schaefer, L.H., and Swedlow, J.R. (2001). A working person's guide to deconvolution in light microscopy. *Biotechniques* 31, 1076–1097.
- Wolf, D.E. (2003). Quantitative digital and video microscopy. In *Methods in Cell Biology*, G. Sluder and D.E. Wolf, eds. (London: Elsevier), pp. 319–339.
- Zucker, R.M., and Price, O. (2001). Evaluation of confocal microscopy system performance. *Cytometry* 44, 273–294.

Please cite this article as:

Waters, J.C., and Swedlow, J.R. (2007). Interpreting Fluorescence Microscopy Images and Measurements. In *Evaluating Techniques in Biochemical Research*, D. Zuk, ed. (Cambridge, MA: Cell Press), <http://www.cellpress.com/misc/page?page=ETBR>.